Postprint of: Włodarski W., Experimental investigations and simulations of the microturbine unit with permanent magnet generator, Energy, Vol. 158 (2018), pp. 59-71, DOI: 10.1016/j.energy.2018.05.199

Experimental investigations and simulations of the microturbine unit with permanent magnet generator

Wojciech Wlodarski

Gdansk University of Technology, Faculty of Mechanical Engineering, Department of Energy and Industrial Apparatus, Narutowicza 11/12, 80-233 Gdansk, Poland

Abstract

In dispersed power generation, low power devices are used for local combined generating of heat end electric power. There are developing concepts of micropower plants with electric generators driven by steam or gas microturbines. The paper presents the results of an experimental investigations of the microturbine set consists of the turbine with partial admission, permanent magnet generator and three phase AC-to-DC rectifier. The microturbine was designed for steam of HFE7100 as a working medium. The dynamic behavior of the microturbine unit was experimentally examined. Microturbine unit was tested during changes of the parameters of the working medium or the electrical load. Experiments were performed with compressed nitrogen as a working medium. The dynamic model of microturbine unit was developed. The examples of the comparison between experiment results and simulations are shown and discussed in the paper.

Keywords:
micro power generation, microturbine, microturbine dynamics

1. Introduction

In the distributed power engineering, relatively low power devices are used for local production of electric power and heat [1]. At present, concepts of micro power plants are being developed in which electric power is generated

Email address: wwlodar@pg.edu.pl (Wojciech Wlodarski)

in microturbine sets consisting of electric current generator driven by thermal microturbine [2]. For this purpose, both gas [3], [4], [5], [6] and steam (vapour) [7], [8], [9], [10], [11] microturbines are used. In cases when the electric power production bases on low-temperature heat sources, the steam microturbines work in installation in which the ORC (Organic Rankine Cycle) is executed [12]. ORC technology is known primarily from large-scale units dedicated to geothermal [13], oceans ([14] or solar [15] energy sources (as evidenced by the trading offers of Ormat Technologies and Turboden) and waste heat recovery systems from energy or technology processes. In this case, apart from the commercially available systems offered by the previously mentioned companies, the literature also shows an original approach to the issue of heat recovery [16], [17]. Recently, with the intensive development of the distributed energy sector in the European Union, ORC technology is also perceived as a prospective technology for units with a household scale - micro-cogeneration systems [18], [19]. The "micro" scale increases the construction and technological challenges. In many research centers are carried out both intensive work on dedicated, modern constructions of compact heat exchangers, signaled in [20], [21], [22] as well as steam engines. In the case of engines, volumetric [23], [24], [25] and turbine engines are developed in parallel [26], [27], [28]. An extensive literature review in this area provides [29].

Microturbine sets are already present in offers of many companies acting on the energy market. Nevertheless, research activities are still in progress to improve the efficiency and reliability of these devices, as well as to decrease their production costs. Difficulties faced when designing and manufacturing microturbine sets are related with, among other factors, miniaturisation of their structural components, high rotational speed, and/or microturbine dynamics and control problems.

A microturbine set is designed for operation in given conditions, i.e. at given thermodynamic parameters of the working medium supplied to the turbine, and given electric load of the turbine. A set of these parameters bears the name of design or calculation parameters. However, during its operating life time the microturbine set can work in conditions differing from those defined by the calculation parameters, for instance due to change of working medium parameters and/or electric load of the turbine set. In such situations, the turbine set will work at partial load or overload, also its rotational speed will be subject to change. Not all of the above changes are permissible, taking into account limitations concerning such factors as: the

strength of rotating turbine and generator components, the durability of generator armature winding, and the need to ensure proper voltage and current parameters of the generated electric power. A possibility of operation in such conditions should be taken into account at the microturbine set design stage. The published results of experimental examination usually refer to steady-state microturbine operation [30], [31], [32], [33]. Changes of operating parameters can also take a dynamic course (for instance, as a result of connecting or disconnecting electric energy receivers). Works can be found in the literature which analyse the dynamics of microturbine sets. Many of them focus on issues relating to bearings and vibrations of microturbines [34], [35], [36], [37]. Experiments showing microturbine sets operation in dynamically changing conditions are rare [38], [39], [40].

An accurate model of the microturbine set is required to analyze the mentioned impacts. Some works describe simulation tests of microturbine sets [41], [42], [43], [44], [45]. Unfortunately, most of them deal with gas microturbines, which makes it difficult to draw conclusions on the operation of other types of microturbine sets from the presented results. There are no works in the literature which would present experiment validated simulation results, and describe, in both qualitative and quantitative way, the performance of the steam microturbine set in changing operating conditions.

Dynamic models, presented in the literature, usually in detail describe all components of microturbine sets: turbines [46], [47], [48], [49], electric current generators [50], [51], [52], rectifying or rectifying/inverter systems [53], [54], [55]. Microturbine set can be modelled by combination of generic equations of all elements. This approach is proper from the accuracy point of view, but in some practical applications could be difficult in performing. Physical model of an object consisting of three connected elements is complicated and contains a large number of coefficients. There are two possible way to obtain values of model coefficients: data received from the device manufacturer or experimental identification. Detailed devices specifications sometimes are not delivered or are delivered as a confidential data. The identification process of microturbine set requires experimental tests of all elements separately. For example, for identify generator and rectifier it is necessary to measure alternating current parameters. Due to the high frequency of electric current, the data acquisition system requirements are increasing. For identify turbine, it is necessary to test it on the special test rig equipped with torque measurement system. In some cases it could be difficult or even impossible. For example, some microturbine sets are designed and delivered as an

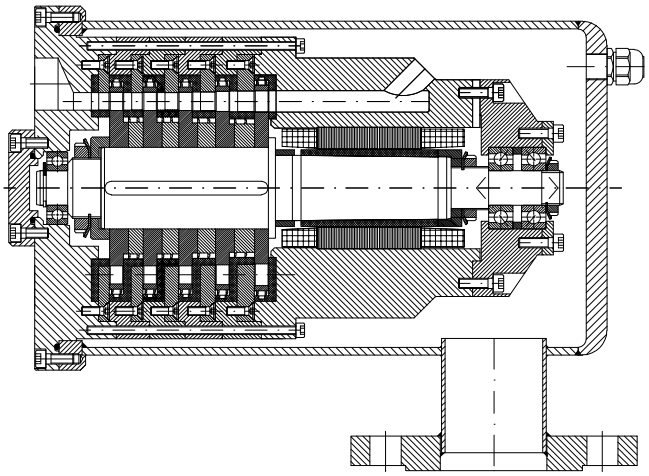

Figure 1: The axial cross-section through the microturbine set

integrated devices with turbine and generator rotors mounted on one shaft and enclosed in a hermetic casing [33], [40]. For mentioned devices it is only possible to measure working medium parameters at the turbine inlet and outlet, electric power parameters and rotational speed. It is not enough for performing identification process for model taking into account full knowledge of microturbine set internal work. In such a situation, it seems that the use of the empirical model may be the right approach.

This paper presents the microturbine set simplified model, where the structure is determined by the observed relationship among experimental data. Model parameter values were determined based on experiments. The proposed model is intended for use in technical applications, when it is not possible to perform separate tests of elements of the object under consideration.

2. Microturbine set

The paper describes the performance of the microturbine set with permanent magnets. The set is assumed to be supplied with the vapour of low-boiling medium HFE 7100 as the working medium. The axial cross-section through the microturbine set is shown in Figure 1.

The set comprises a 5-stage axial microturbine which drives a three-phase generator with permanent magnets. A characteristic feature of the turbine

Figure 2: Microturbine set with disassembled hermetic casing and the casing alone

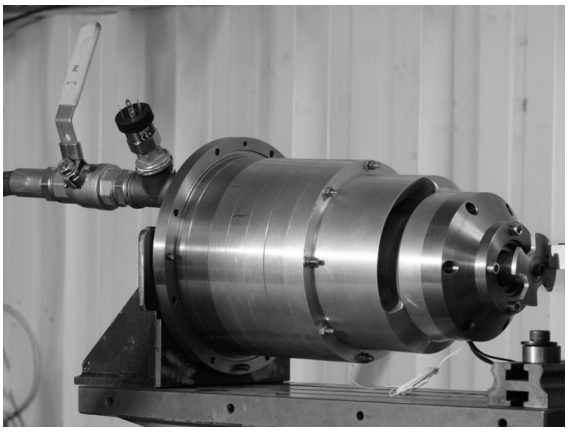

Figure 3: Microturbine set during test runs

is partial admission in all five stages. The turbine rotor and the generator rotor are mounted on one shaft supported on ceramic rolling bearings. The electric current generator is situated on the low-pressure side of the turbine. The generator stator is mounted in the turbine exit body, while the rotor is fastened on the conical surface of the turbine shaft. Tightness of the turbine is ensured by hermetic casing screwed to the turbine inlet body. A photo of the microturbine set with disassembled casing and the casing alone are shown in Figure 2. The set (without hermetic casing) during test runs is shown in Figure 3.

Basic design parameters of the microturbine are given in Table 1.

The electric current generator was the three-phase generator with permanent magnets in rotor. The generator equivalent circuit data is provided

Table 1: Design parameters of the microturbine

turbine power	2990 W
medium mass flow rate	0,1687 kg/s
pressure at turbine inlet	1200 kPa
temperature at turbine inlet	162 °C
pressure behind the turbine	118,6 kPa
temperature behind the turbine	126,9 °C
rotor speed	8073 rpm

Table 2: Generator equivalent circuit data

description	value
motor voltage	215 V
rated frequency	367 Hz
rated current	6 A
inverter output voltage	215 V
series choke	0,3 mH
phase stator resistance	1,84 Ω
phase stator leakage reactance	2.,91 Ω
phase main field reactance	10,7 Ω
synchronous phase motor reactance	13,6 Ω
magnet wheel voltage	184 V
maximum inverter output voltage (phase-to-phase)	380 V
motor main field inductance	4,63 mH
motor leakage inductance	1,26 mH

in Table 2.

The alternating current from generator phases is converted to direct current in the bridge rectifier using Lamina diodes type R51-100-12-N7-DA1 and R51-100-12-R7-DA1 as the switching elements. Rectifier unit is shown in Figure 4.

The considered microturbine set was tested without any voltage regulation. Control system have to be considered for completing energy generation. Possible topology could be composed by a diode rectifier associated with a boost converter [56]. Schematic diagram of the microturbine set with diode rectifier assisted by the boost converter is shown in the Figure 5.

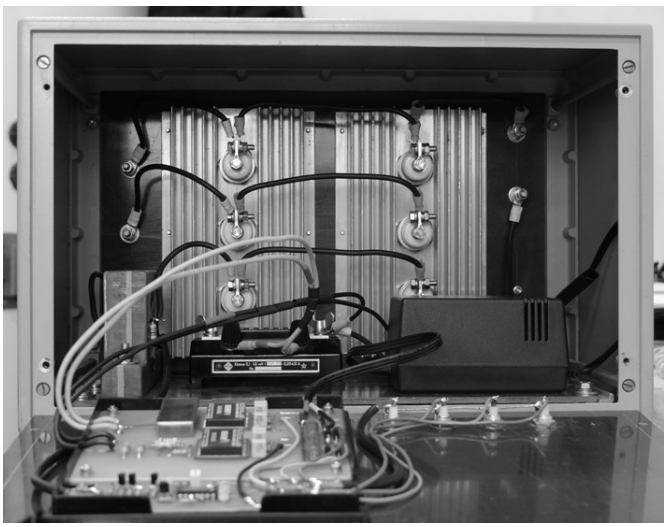

Figure 4: Rectifier unit

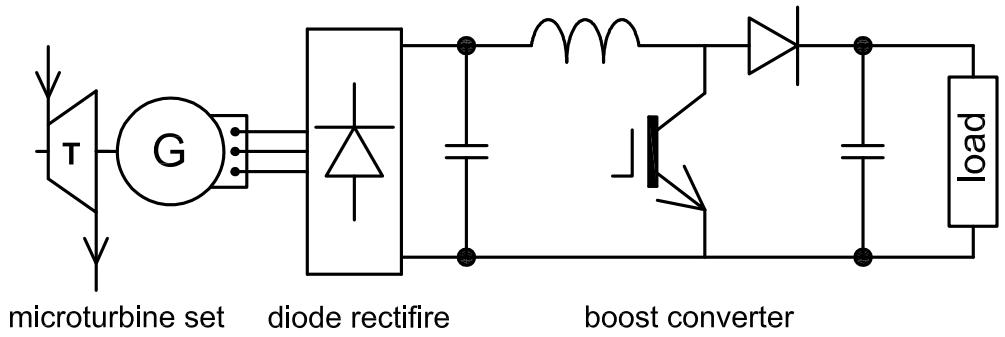

Figure 5: Schematic diagram of the microturbine set with diode rectifier assisted by the boost converter

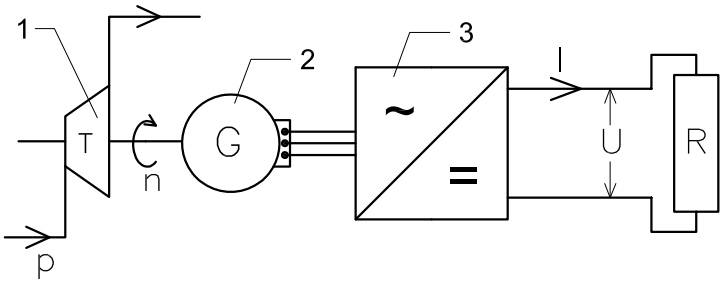

Figure 6: Schematic diagram of the test rig, 1 - microturbine, 2 - electric current generator, 3 - rectifying system, R - resistor in which the electric energy is converted to heat, p - pressure at turbine inlet, n - rotor speed, U - electric voltage, I - electric current

3. Experimental examination of the microturbine set

The microturbine set was examined on the laboratory test rig designed and manufactured for this purpose. Due to microturbine set construction it was impossible to examine turbine and generator separately. During the experiments described in the paper, the turbine was supplied with compressed nitrogen. After leaving the turbine, the working medium flowed directly to the environment. A schematic diagram of the test rig is shown in Figure 6. The three-phase current generator is connected via phase conductors with the rectifying system which converts the alternating current to direct current. On the direct-current side, the rectifier is connected to a resistor in which the electric energy is converted to heat. Changes of the microturbine set operation state were executed by changing the working medium pressure at turbine inlet, or by changing the resistance of the resistor which loads the generator.

Pressure at turbine inlet was measured using the Trafag sensor type: 8472.79.5717. Electric current and voltage were measured using the device based on Burr-Brown isolation amplifiers type: 3656AG and 3656BG. Rotational speed was specified using Optek slotted optical switch type OPB960. Electrical parameters of the microturbine set (voltage, electric current) were measured on the direct-current side. Systematic errors of the pressure measurements was estimated at $\pm 0{,}06$ bar, electric current measurements at $\pm 0{,}04$ A, voltage measurements at $\pm 4{,}8$ V. Rotational speed systematic errors depended on speed value, e.g. at 3000 rpm was equal ± 10 rpm, at 13000 rpm was equal ± 178 rpm. Random errors have not been determined.

Detailed documentation of the microturbine set and the laboratory test

rig can be found in: [38], [40].

A series of experimental tests were performed to study the performance of the microturbine set in changing operating conditions, expected in real microturbine operation.

In the first stage of examination, parameters of steady-state operation of the microturbine set were recorded. The collected data provided opportunities for working out static characteristics relating such parameters as: working medium pressure at turbine inlet, rotational speed of the rotor, voltage, electric current, power, as well as the resistance of the electric energy receiver.

In the second stage, the performance of the microturbine set was recorded in dynamically changing operating conditions. The observed performance issues included responses to step changes of the working medium pressure at turbine inlet and the resistance of the generator's load resistor.

The recorded results have provided opportunities for evaluating static and dynamic performance of the examined microturbine set in both qualitative and quantitative terms.

A detailed description and results of the performed experimental tests can be found in [40]. Selected sample results are shown in figures: 7, 8, 9 and 10.

Figure 7 shows the rotational speed of the microturbine set as a function of working medium pressure at turbine inlet, for different load resistant. The turbine exit pressure was constant and equal to the ambient pressure. The obtained characteristics have a linear shape. With the increasing working medium pressure or the load resistant, the rotational speed also increases.

Figure 8 shows the rotational speed of microturbine rotor as a function of load resistance, for constant inlet pressure values of the working medium supplied to the turbine. Increasing the resistance or the inlet pressure results in the increase of the rotational speed. It is noteworthy that these characteristics have clearly nonlinear shape.

Figure 9 shows the time-histories of turbine inlet pressure, rotational speed of rotor, voltage, electric current of the microturbine set, recorded after increasing the opening of the turbine supply valve. The test was performed for constant load resistance. As a result of the turbine inlet valve setting change, rapid pressure increase is observed, which is followed by gradual increase of the rotational speed of rotor. This is accompanied by the increase of electric parameters of the microturbine set: voltage and electric currentr. What is worth mentioning here is relatively long time (of about 8 sec) needed

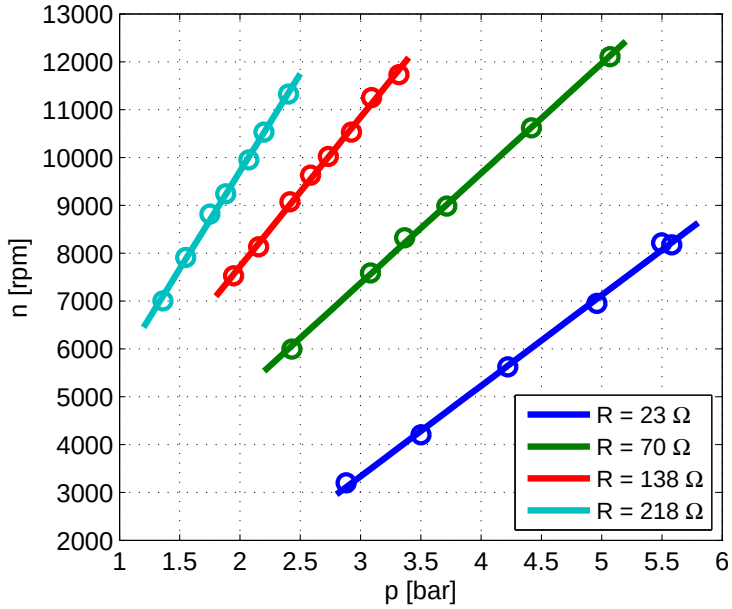

Figure 7: Rotational speed n of the microturbine set as a function of working medium pressure p, for different load resistance R

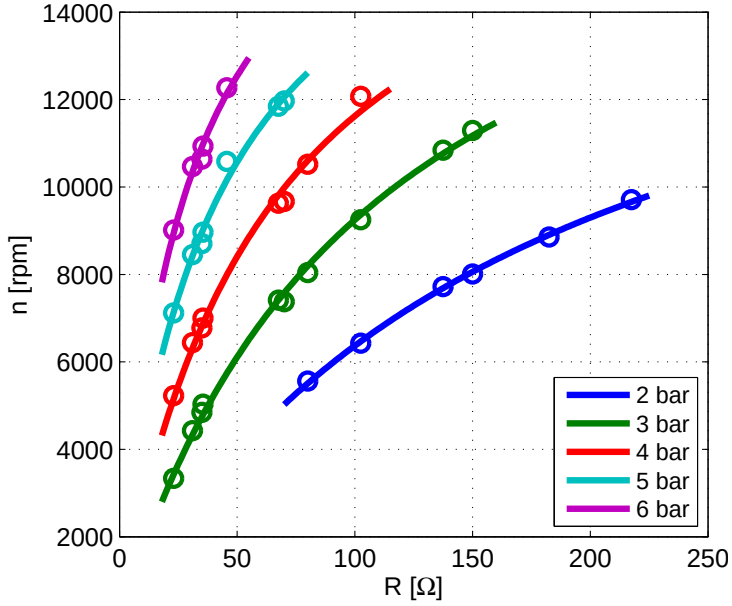

Figure 8: Rotational speed n as a function of load resistance R, for different working medium pressure values at turbine inlet

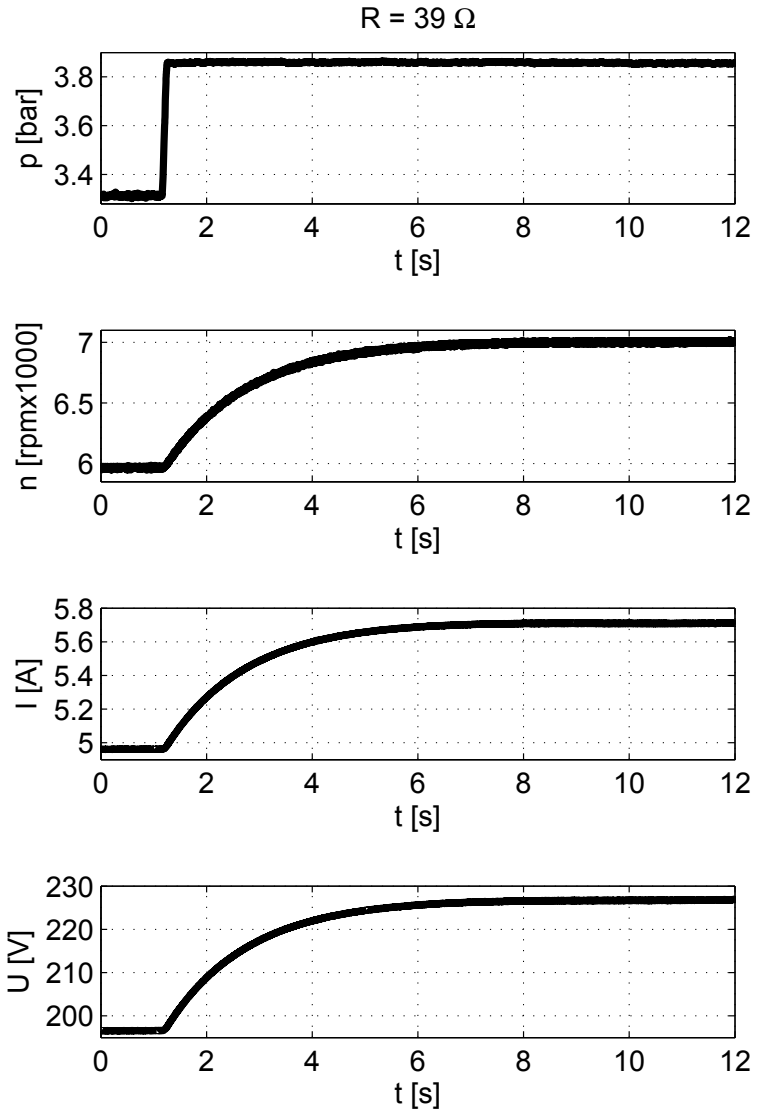

Figure 9: Rotational speed n, electric voltage U, electric current I as a function of time t, after pressure p at turbine inlet changes, for constant load resistance, equal to $R = 39\,\Omega$

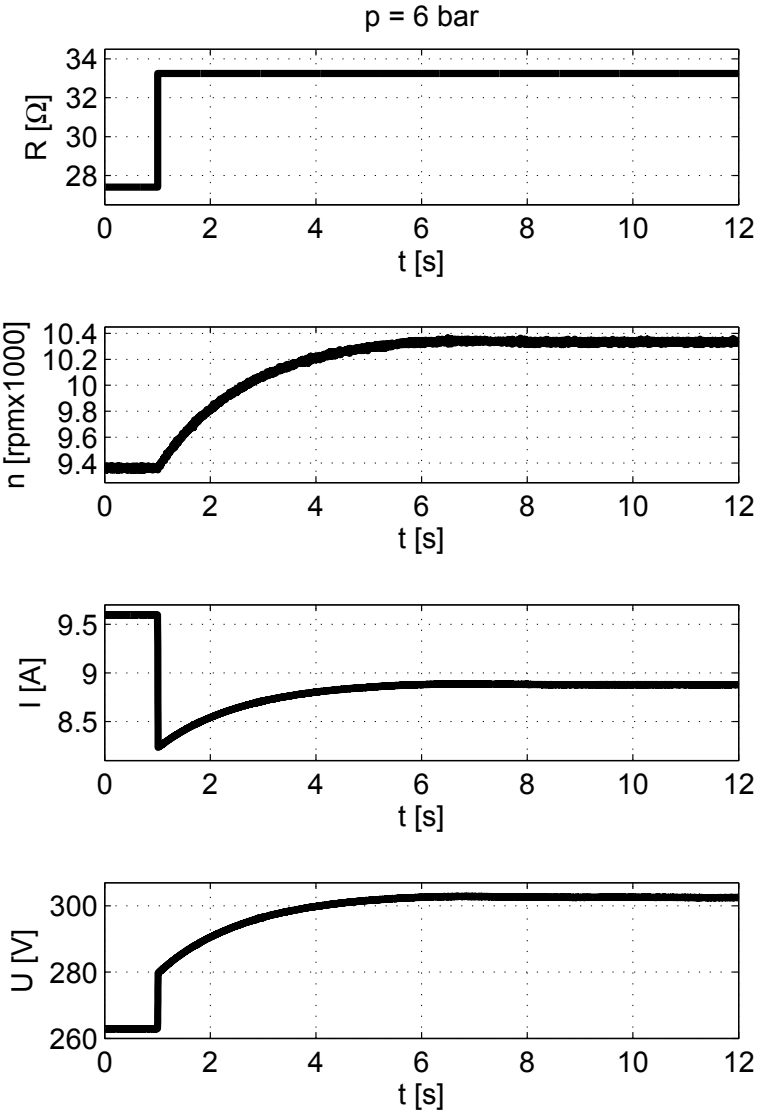

Figure 10: Rotational speed n, electric voltage U, electric current I as a function of time t, after load resistance R changes, for constant pressure p at turbine inlet, equal p = 6 bar

for stabilisation of new parameters of microturbine set operation.

It is also noteworthy that the response of all the above-mentioned parameters to pressure change was similar to the response of the proportional element with first order inertia to step excitation.

Figure 10 shows the results of the test recording the microturbine set response to resistance changes of the generator's load resistor. The structure of the used power reception system made it possible to switch between load resistors during microturbine operation. This way, step changes of load resistance were generated. The test was performed for constant working medium inlet pressure. After the step change of load resistance, the rotational speed gradually increased. The recorded time-history of the rotational speed of rotor was similar to the response of the proportional element with first order inertia to step excitation. The response of the electric part of the microturbine set was different in nature and can be divided into two stages. In the first stage, directly after the step change of resistance, the changes of voltage and electric current had the same rapid course. The voltage increased, while the electric current and power decreased. In the second stage, the observed gradual increase of rotational speed of rotor was accompanied by gradual change of electric parameters of the microturbine set.

4. Identifying the microturbine set

The results of experimental examination were used to develop the mathematical model of microturbine set. The model was expected to be able to predict correctly the microturbine set performance after change of operating conditions.

A schematic diagram of the model of microturbine set is shown in Figure 11. The assumed input signals of the model are: the working medium pressure at turbine inlet and the resistance of electric energy receiver. The turbine exit pressure is assumed constant. The assumed outlet signals are: the rotational speed of microturbine rotor, and the electric current and voltage measured behind the rectifying unit.

Figure 12 shows a simplified block diagram of the model of microturbine set. Developing the mathematical model of the analysed system requires the information on time relations between the rotational speed signal and the signals of turbine inlet pressure and load resistance, as well the relations between the electric current, the rotational speed of rotor and the resistance. The voltage is the product of electric current and resistance.

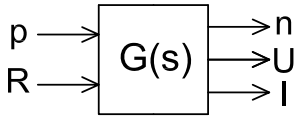

Figure 11: Schematic diagram of the model of microturbine set: G(s) - transmittance, p - pressure at turbine inlet, R - resistance of electric energy receiver, n - rotational speed, U - electric voltage, I - electric current

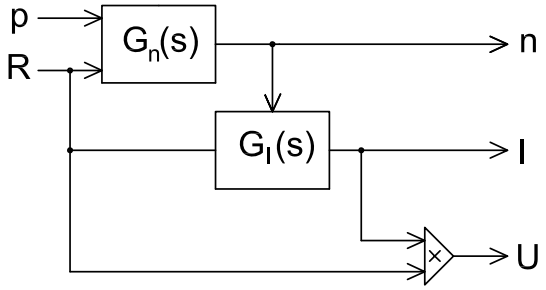

Figure 12: Simplified block diagram of the model of microturbine set: p - pressure at turbine inlet, R - resistance of electric energy receiver, n - rotational speed, U - electric voltage, I - electric current, $G_n(s)$, $G_I(s)$ - transmittances

The transmittance $G_n(s)$, defining the relation between rotational speed n, pressure p, and load resistance R, was assumed to be a linear relation comprising two proportional elements with first order inertia, connected in parallel:

$$G_n(s) = G_{np}(s) + G_{nR}(s) + A_n, \tag{1}$$

where:

$G_{np}(s) = \frac{K_p}{1+T_p \cdot s}$ - transmittance defining the relation between the output signal of rotational speed n and the input signal of inlet turbine pressure p,

$G_{nR}(s) = \frac{K_R}{1+T_R \cdot s}$ - transmittance defining the relation between the output signal of rotational speed n and the input signal of load resistance R,

A_n - constant value.

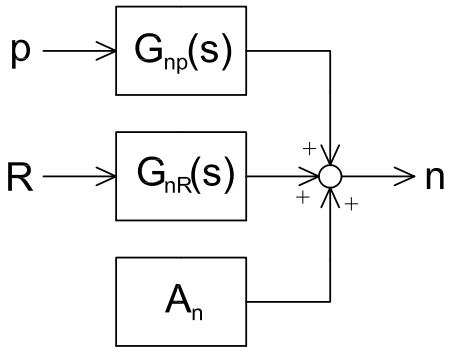

Figure 13: Simplified block diagram of the model fragment: $G_{np}(s)$, $G_{nR}(s)$ - transmittances, A_n - constant value

A simplified block diagram of the model fragment describing the relation between the rotational speed signal and the signals of turbine inlet pressure and generator load resistance is shown in Figure 13.

The model under consideration assumes a linear relation between inlet pressure, load resistance and rotational speed. According to experimental characteristics in Figure 7 the relation between rotational speed and inlet pressure can be treated as linear in a wide range. The relation between rotational speed and load resistance (Figure 8) is clearly non-linear, so this model could describes the microturbine set performance within a small range of load resistance changes.

The values of transmittance $G_n(s)$ coefficients were obtained due to experiment results. Data for the inlet turbine pressure range from 3 bar to 6 bar and the load resistance range from 27 Ω to 39 Ω were used for identifying the microturbine set. A solution was found with a minimum square error, from data collected from mentioned operation conditions ranges:

- $K_p = 1885\ rpm/bar$,
- $K_R = 131{,}6\ rpm/\Omega$,
- $T_p = T_R = 1{,}48\,s$,
- $A_n = 5367\,rpm$.

Electric part of the microturbine set consists of permanent magnets synchronous motor connected with bridge rectifier using diodes as the switching

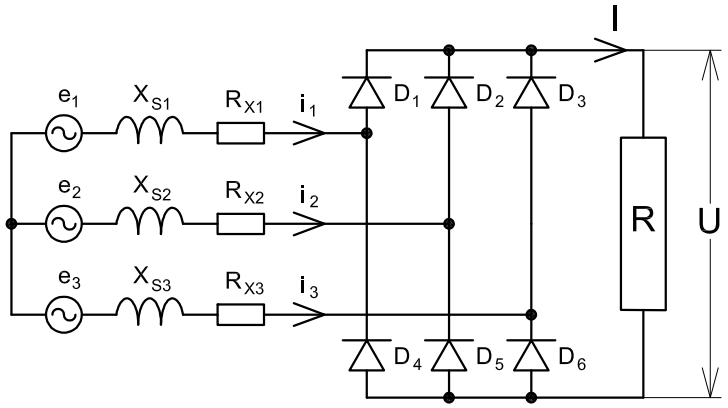

Figure 14: Equivalent circuit diagram of the electric part of the microturbine set: $e_{1,2,3}$ - phase electromotive forces, $X_{S1,2,3}$ - phase synchronous reactances, $R_{X1,2,3}$ - phase stator resistances, $i_{1,2,3}$ - phase electric currents, $D_{1,2,3,4,5,6}$ - rectifier diodes, I - electric current, U - voltage, R - resistance of electric energy receiver

elements. Equivalent circuit diagram of the electric part of the microturbine set are provided in Figure 14. It is possible to model this device by generic equations, but identification process requires complicated measurement operations, which increase the time and cost of testing. The simplified approach has been proposed, in which the microturbine set connected with the rectifier was assumed to constitute one element, for which the empirical model have to be worked out. With this approach, a microturbine set would be treated as a source of direct current electric energy. This would enable to omit detailed description of electrical processes taking place on the alternating-current side and would limit required electrical measurements to direct current. From the point of view of operating such a device, it is important to know the values of input and output signals. Knowledge of indirect signals, such as a torque on a turbine shaft or electrical parameters in the individual phases of a generator, is important at a design stage of a microturbine set, but it does not have to be necessary for a final user.

Electrical energy losses in the mentioned device are composed of the following elements: losses in generator winding and losses in rectifier diodes. Instead of identifying the individual loss components separately, it was proposed to introduce a new equivalent term that would include total energy losses. As a name for this term, it was proposed "equivalent device resistance". Reactance and diodes losses depend on the frequency [55], [57] so

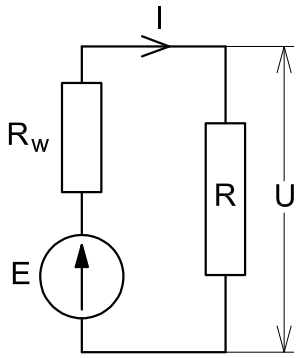

Figure 15: Simplified equivalent circuit diagram of the DC electric part of the microturbine set: E - equivalent DC source potential, R_w - equivalent device resistance, I - electric current, U - voltage, R - resistance of electric energy receiver

equivalent device resistance should be specified as a function of frequency or rotational speed of a microturbine.

Equivalent circuit diagram of the simplified electric part of the microturbine set are provided in Figure 15. It is a DC circuit and refers to the electrical parameters observed in the DC part of the microturbine set. It consists of equivalent device resistance, resistance of electric energy receiver and equivalent DC source potential. The "equivalent DC source potential" is introduced term, which results from the sum of electromotive forces of individual generator phases. The values of equivalent DC source potential and equivalent device resistance depend on the operating conditions and should be specified so that the system response would be the same as the original device.

Figure 16 presents a schematic diagram of the model fragment representing the relation between the electric current in the DC part of the microturbine set, the rotational speed of microturbine rotor, and the sum of load resistance and equivalent device resistance.

The relation between the equivalent DC source potential, the equivalent device resistance and the rotational speed of rotor was determined based on experimental results. Responses to step changes of the resistance of the load resistor were recorded. The diagram of these tests is shown in the Figure 17. During operation of the microturbine set, at time t_0, the load resistance was changed from R_1 to R_2. Due to the large difference between the inertia of the mechanical and electrical parts of the microturbine set it was assumed that at the time when the electric current and voltage changed from I_1 to I_2

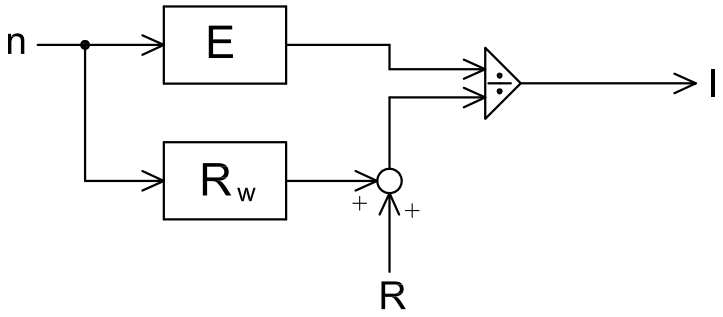

Figure 16: Schematic diagram of the model fragment: I - DC current, n - rotational speed, R - load resistance, R_w - equivalent device resistance, E - equivalent DC source potential

and from U_1 to U_2 respectively, the rotational speed did not change. If the rotational speed did not change, then also the equivalent DC source potential and equivalent device resistance did not change:

$$E = U_1 + I_1 \cdot R_w = U_2 + I_2 \cdot R_w \tag{2}$$

Equation 2 allows to calculate the values of the equivalent DC source potential. By converting this equation it is possible to calculate equivalent device resistance:

$$R_w = \frac{U_1 - U_2}{U_1 \cdot R_2 - U_2 \cdot R_1} R_1 \cdot R_2. \tag{3}$$

Figure 18 shows the determined relation between the equivalent DC source potential and the rotational speed of microturbine rotor. Points obtained from the experiment were approximated by a second-order polynomial:

$$E = 8,537 \cdot 10^{-7} \cdot n^2 + 0,0294 \cdot n + 28,82. \tag{4}$$

The performed experiments have revealed clear dependence of the equivalent device resistance on the rotational speed of rotor (Figure 19). The measured data were approximated by a quadratic function:

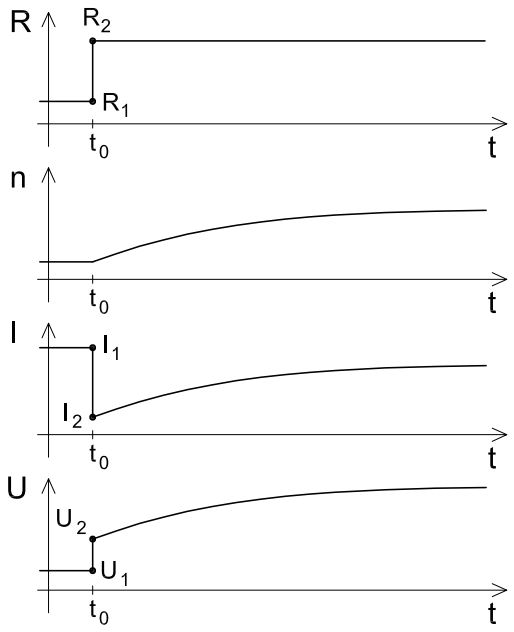

Figure 17: Rotational speed n, electric current I and voltage U, electric current I as a function of time t, after load resistance R change

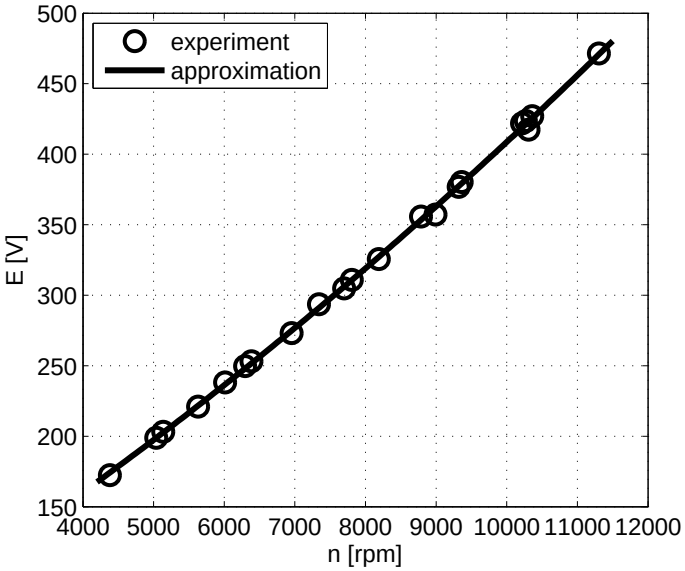

Figure 18: Equivalent DC source potential E as a function of rotational speed n

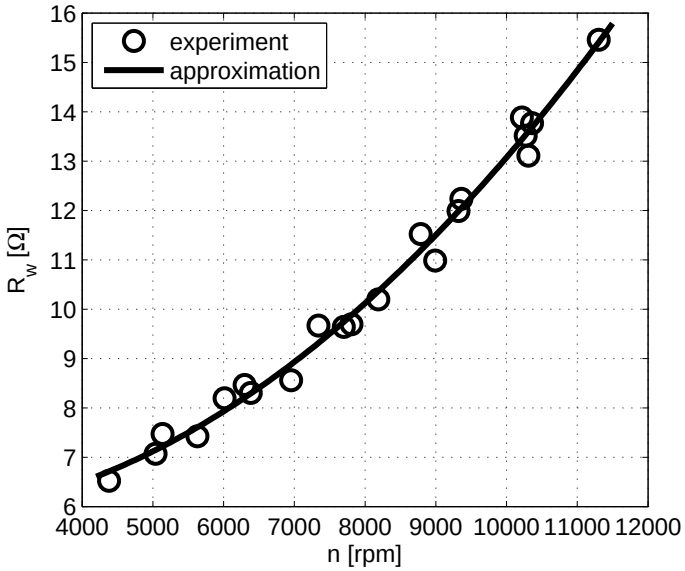

Figure 19: Equivalent device resistance R_w as a function of rotational speed n

$$R_w = 9,5221 \cdot 10^{-8} \cdot n^2 - 2,3725 \cdot 10^{-4} \cdot n + 5,9241. \tag{5}$$

The proposed model of electric part of the microturbine set is empirical model. To accept it, it was compared to one of the available theoretical models [58]. This model describes the operation of uncontrolled 3-phase bridge rectifier with resistive and inductive source impedances. The calculations, using a theoretical model, were performed with data from the Table 2. These data were provided by the generator manufacturer and were not experimentally confirmed. Figure 20 shows voltage values as a function of electric current, for different values of rotational speed, obtained from theoretical and empirical model. Calculations were performed for the electric current range between 1 A and 10 A, and rotational speed between 6000 rpm and 12000 rpm, whith is similar to the expected operation area of the microturbine set. The voltages obtained with the theoretical model were lower than those obtained with the empirical model, however, both characteristics were the same in qualitative sense. The maximum value of the relative difference between theoretical and empirical models resulte equals to 16,2 %, the average value equals to 8,3 %. It can be expected that if experimentally obtained generator data were used in the theoretical calculations, these differences

would have lower values.

Complete structure of the developed model of microturbine set is given in the block diagram in Figure 21. This model includes two nonlinear elements which model the relations of the rotational speed with the equivalent DC source potential and the equivalent device resistance.

5. Model validation

A series of calculations were performed to compare the developed model with experimental examination. The model was validated on a different set of observations than used for the identification of the considered microturbine set.

In the first stage the microturbine set model was validated in the operating conditions similar to used for the identification process.

The example results of this comparison are shown in Figures 22, 23, 24 and 25, presenting sample time-histories of the rotational speed of microturbine rotor, and the electric current and voltage, recorded in the experiment and simulated using the developed model for the cases of rapid change of operating conditions. The input data for the calculations were the experimentally recorded values of the turbine inlet pressure and the resistance of electric energy receiver.

Figure 22 shows the microturbine set response to rapid decrease of turbine inlet pressure, from 6 bar to 2,7 bar, during the experiment, while Figure 23 shows a similar response after increasing the pressure from 2,7 bar to 6 bar. In both tests the microturbine set provided power for the electric energy receiver with 33 Ω resistance. After the pressure change, the rotational speed increased gradually from 4300 rpm to 10100 rpm, the voltage from 4,3 V to 8,8 V, and the electric current from 140 A to 299 A. In both tests, the time needed for stabilisation of new parameters of microturbine set operation was approximately equal to 8 sec. The diagrams additionally show the numerically simulated time-histories of rotational speed, voltage and electric current signals.

Figure 24 shows the time-histories of rotational speed, electric current and voltage obtained after experimental step decrease of electric energy receiver's resistance from 39 Ω to 31 Ω. During the test, the working medium pressure at turbine inlet was equal to 4,03 bar. After the load change, the rotational speed decreased gradually from 7340 rpm to 6300 rpm. Directly after the resistance change, the voltage rapidly decreased from 236 V to 223 V

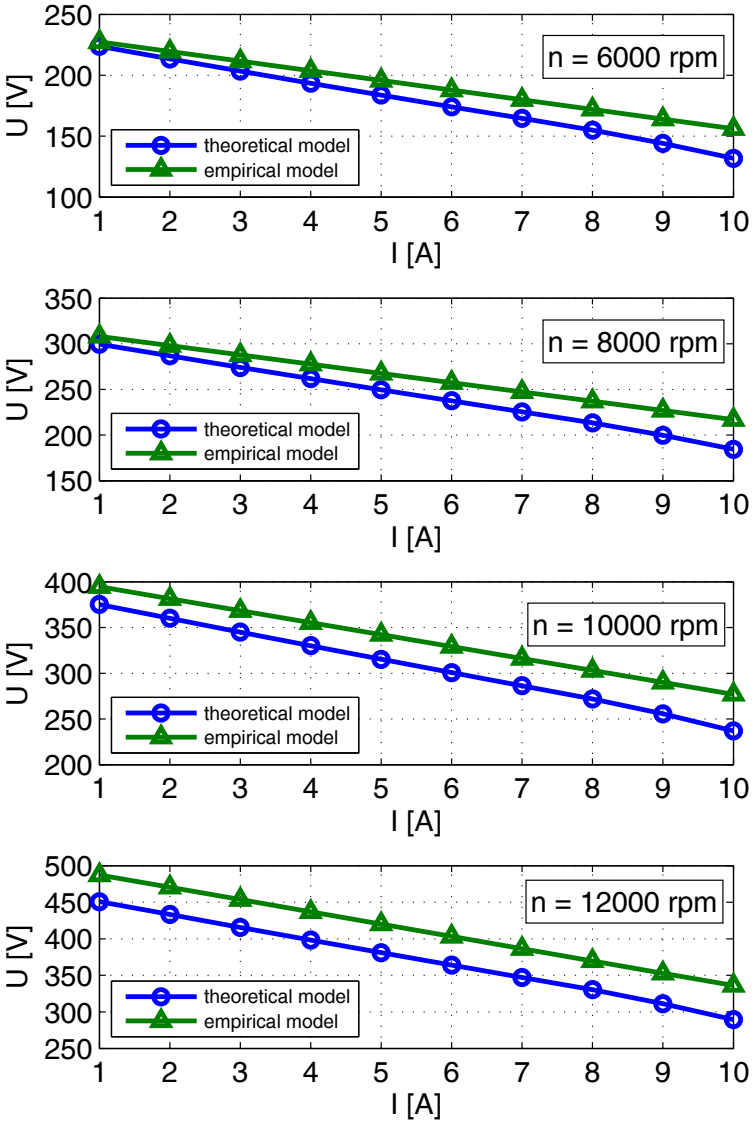

Figure 20: Voltage U as a function of electric current I for different rotational speed n, calculated with theoretical and empirical model

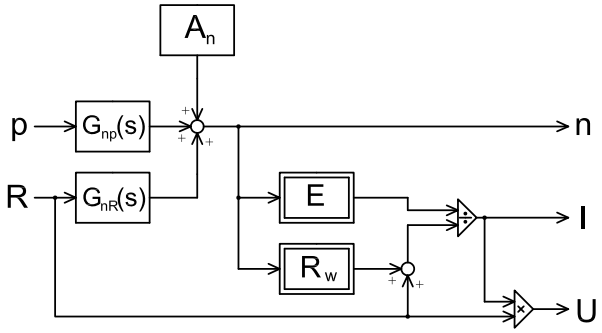

Figure 21: Structure of the developed model of microturbine set: p - input signal of inlet turbine pressure, R - input signal of load resistance, $G_{np}(s)$, $G_{nR}(s)$ - transmittances, A_n - constant value, E - equivalent DC source potential, R_w - equivalent device resistance, n - output signal of rotational speed, I - output signal of electric current, U - output signal of voltage

and then began to decrease slowly to 195 V. The electric current initially increased rapidly from 6 A to 7,4 A and then decreased gradually to 6,45 A. The microturbine set response to step increase of electric energy receiver's resistance from 31 Ω to 39 Ω is shown in Figure 25. In this case, the changes of parameter values went in the opposite direction. The rotational speed increased gradually from 6300 rpm to 7340 rpm, the voltage increased rapidly from 195 V to 206 V and then continued to increase gradually to 236 V, and the electric current decreased rapidly from 6,45 A to 5,23 A, to increase gradually to 6 A. In both tests, the time after the load resistance change which was needed to reach the new steady state was approximately equal to 7 s. The diagrams additionally show the numerically simulated time-histories of rotational speed, voltage and electric current signals.

It is noteworthy that the developed model correctly predicts the state of the microturbine set during changes operating conditions. The parameter values obtained from calculations were close to those recorded experimentally. In the presented examples, the largest difference between simulation and experiment is observed in Figures 24 and 25, in the electric current signals. This relative difference is equal 1,6 %. This difference has been interpreted as the effect of random errors in experimental measurements which were caused by unknown and unpredictable changes in the experiment. These changes may occur in the measuring instruments or in the microturbine set operating conditions.

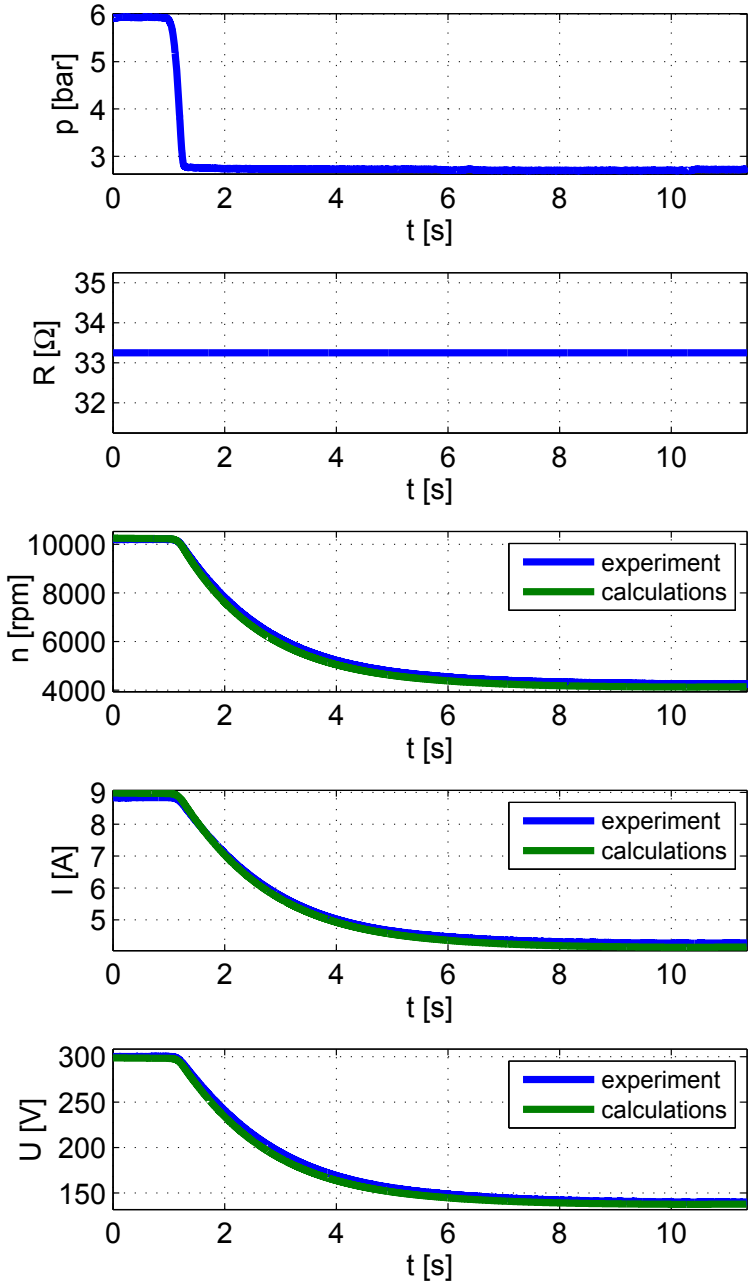

Figure 22: Rotational speed n, electric voltage U and electric current I of the microturbine set as a function of time t, after pressure p at turbine inlet changes, for constant load resistance R, obtained from experiment and calculations

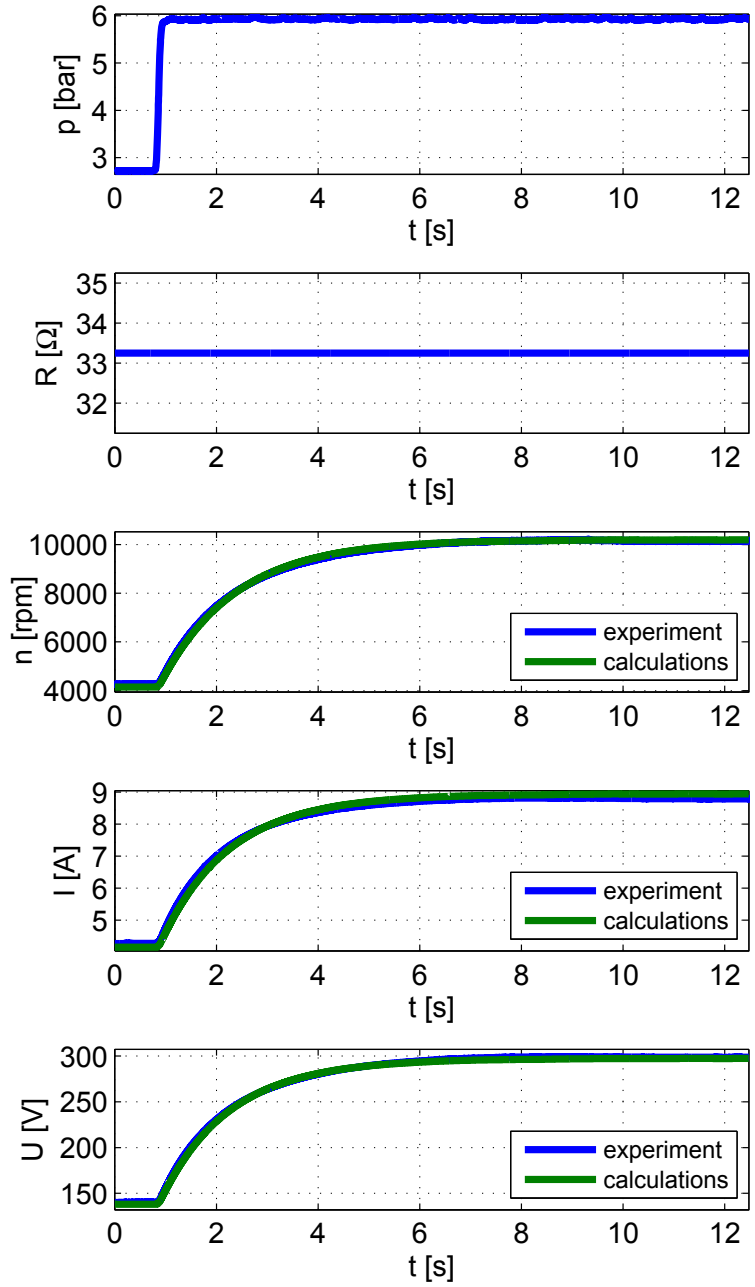

Figure 23: Rotational speed n, electric voltage U and electric current I of the microturbine set as a function of time t, after pressure p at turbine inlet changes, for constant load resistance R, obtained from experiment and calculations

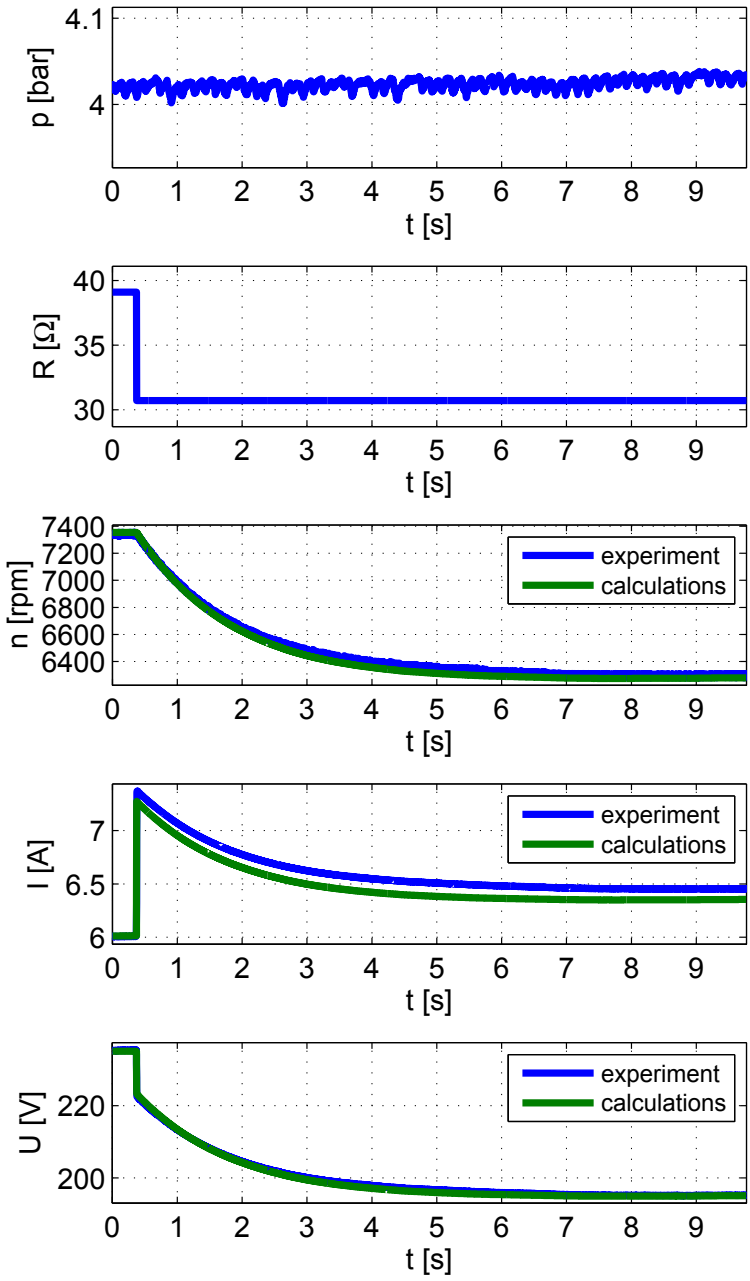

Figure 24: Rotational speed n, electric voltage U and electric current I of the microturbine set as a function of time t, after load resistance R changes, for constant pressure p at turbine inlet, obtained from experiment and calculations

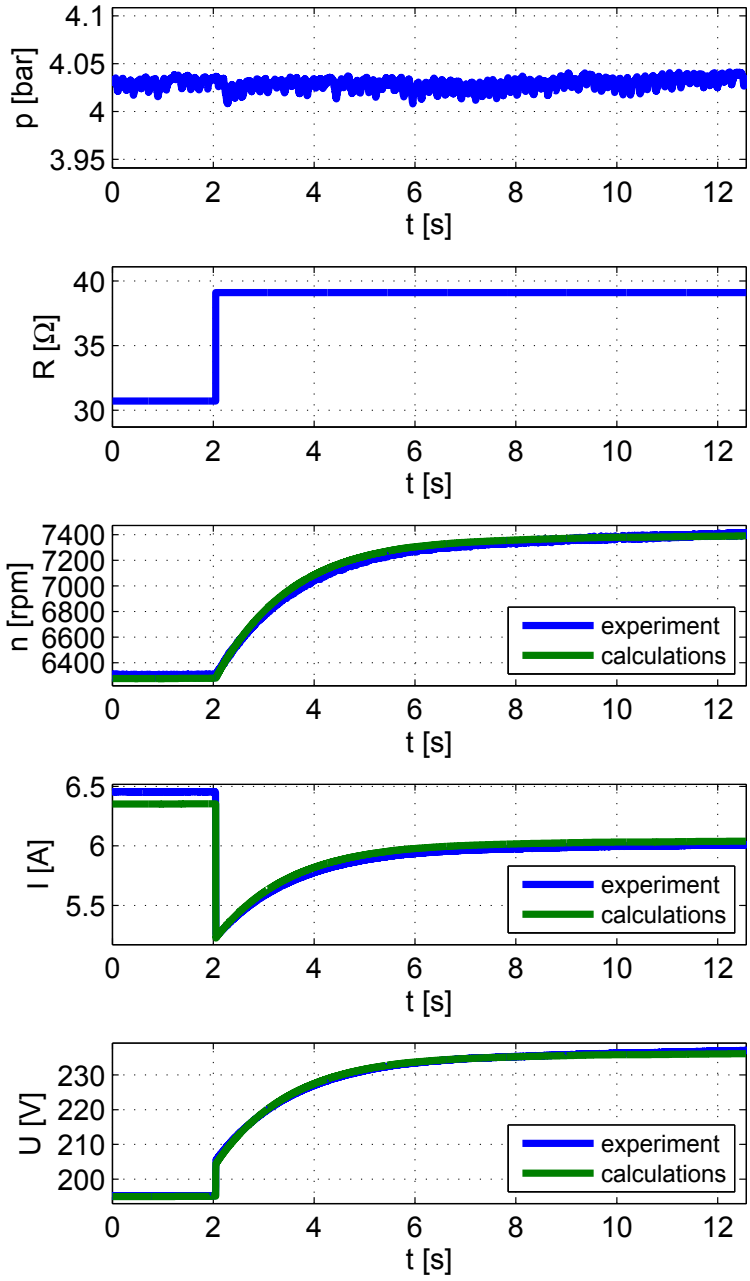

Figure 25: Rotational speed n, electric voltage U and electric current I of the microturbine set as a function of time t, after load resistance R changes, for constant pressure p at turbine inlet, obtained from experiment and calculations

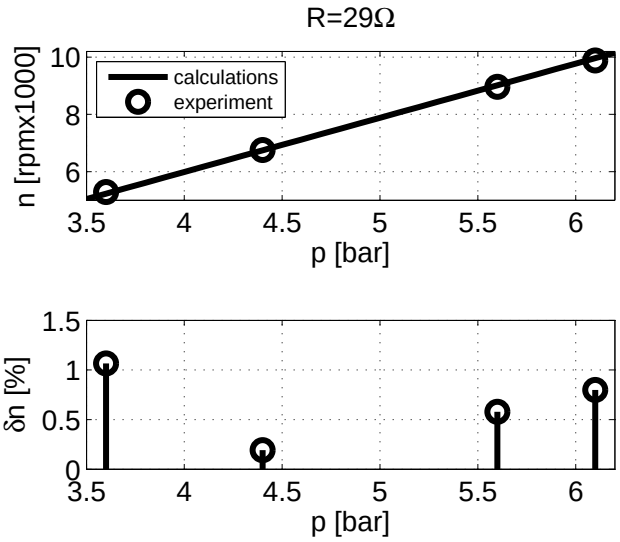

Figure 26: Rotational speed n of the microturbine set as a function of pressure p at the turbine inlet, for constant load resistance $R = 29\,\Omega$ and relative error δn between experiment and calculations

Similar differences were observed in another sets of observations but the magnitude of errors was different and related to different signals. Figures 26, 27, 28, 29, 30 and 31 show rotational speed, electric current and voltage as a function of pressure at turbine inlet, obtained from experiment and calculations, for constant load resistance equal to $29\,\Omega$ and $36\,\Omega$. For this example results the maximum values of relative errors were 2,1 % for rotational speed, 3,3 % for electric current and 1,1 % for voltage.

Mean values of relative errors, from all measurement series, were 0,7 % for rotational speed, 1,2 % for electric current and 0,7 % for voltage.

Obtained results show that developed model provides comparable accuracy with generic equations models. For example, in gas microturbine set models presented in [59] and [60] the errors in the power produced by the generator is less than 5 %.

In the second stage, the microturbine set model was validated in a much wider range of load resistances than used in the identification process. Figures 32, 33 and 34 show rotational speed, electric current and voltage as a function of load resistance, obtained from experiment and calculations, for constant pressure at turbine inlet equal to 4 bar. Additionally, the magni-

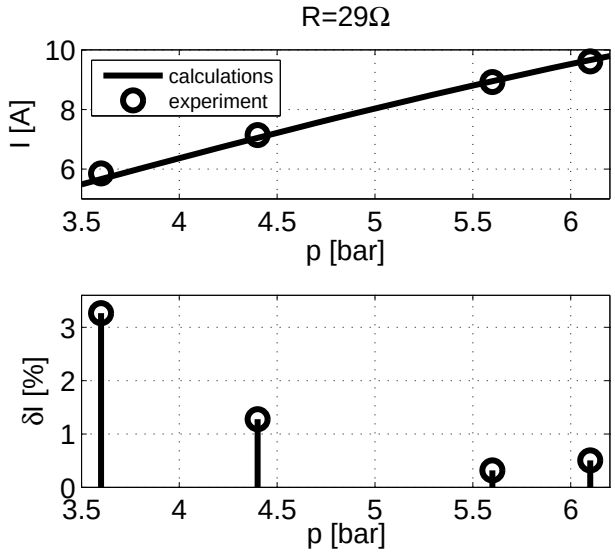

Figure 27: Electric current I of the microturbine set as a function of pressure p at the turbine inlet, for constant load resistance $\mathrm{R} = 29\,\Omega$ and relative error δI between experiment and calculations

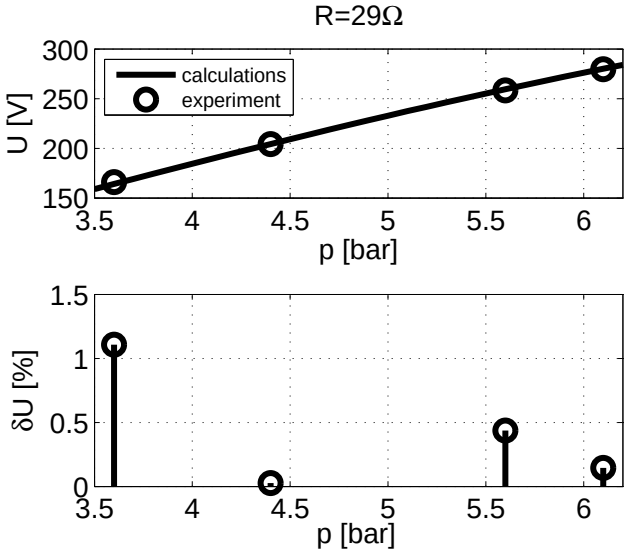

Figure 28: Electric voltage U of the microturbine set as a function of pressure p at the turbine inlet, for constant load resistance $\mathrm{R} = 29\,\Omega$ and relative error δU between experiment and calculations

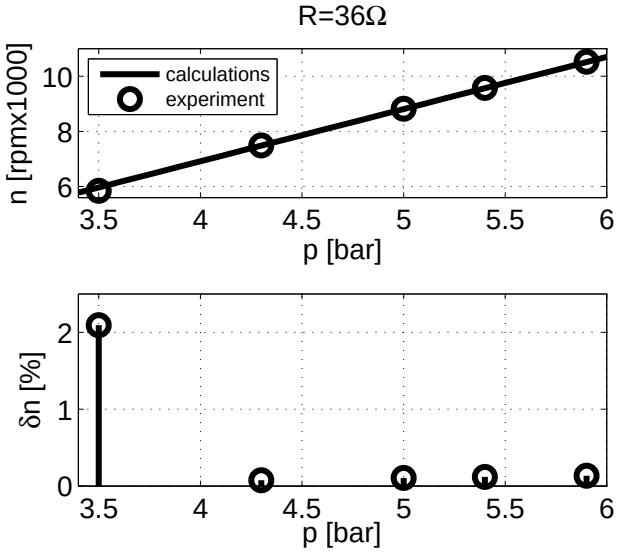

Figure 29: Rotational speed n of the microturbine set as a function of pressure p at the turbine inlet, for constant load resistance $\mathrm{R} = 36\,\Omega$ and relative error δn between experiment and calculations

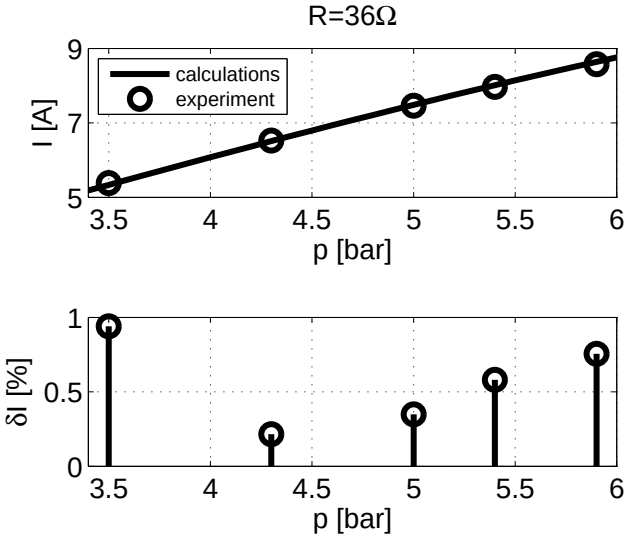

Figure 30: Electric current I of the microturbine set as a function of pressure p at the turbine inlet, for constant load resistance $\mathrm{R} = 36\,\Omega$ and relative error δI between experiment and calculations

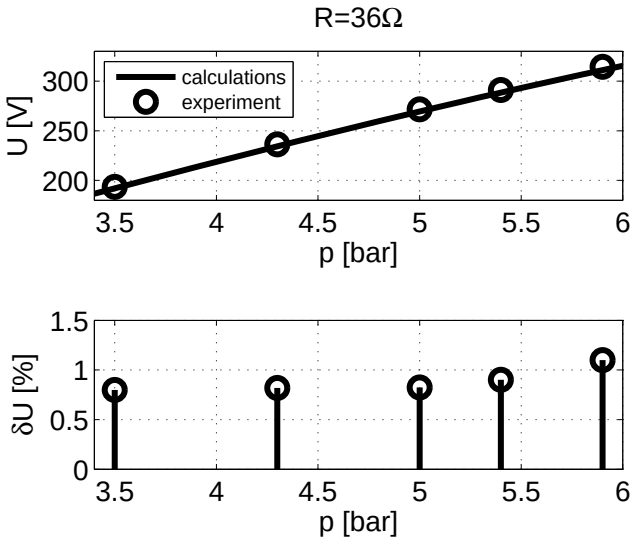

Figure 31: Electric voltage U of the microturbine set as a function of pressure p at the turbine inlet, for constant load resistance $R = 36\,\Omega$ and relative error δU between experiment and calculations

tudes of relative errors were plotted. In the range of small resistance values relative differences between simulation and experiment did not exceed 5 %. As the resistance increased, the sizes of errors also increased. For load resistance equal to 103 Ω, values of relative errors were equal to 30,2 % for rotational speed, 35,6 % for electric current and 35,6 % for voltage.

The presented results confirm that, despite considerable simplifications, the use of the proposed model of microturbine set ensures a few percent accuracy of results, within a relatively large range of inlet pressure, but in a small range of load resistance. Increasing the resistance range increases the inaccuracy of the results above the acceptable level for typical engineering calculations. This is because the model adopts a linear relation between the load resistance and the rotational speed. In fact, this relation is non-linear. In order to extend the scope of applicability of the model, one may consider modifying by replacing the linear relation, between the load resistance and the rotational speed, with a non-linear relation.

Based on the results of the validation calculations the microturbine set operation range, in which the model is reliable, was determined from the inlet pressure equals 3 bar with the power equals 570 W up to pressure 6 bar

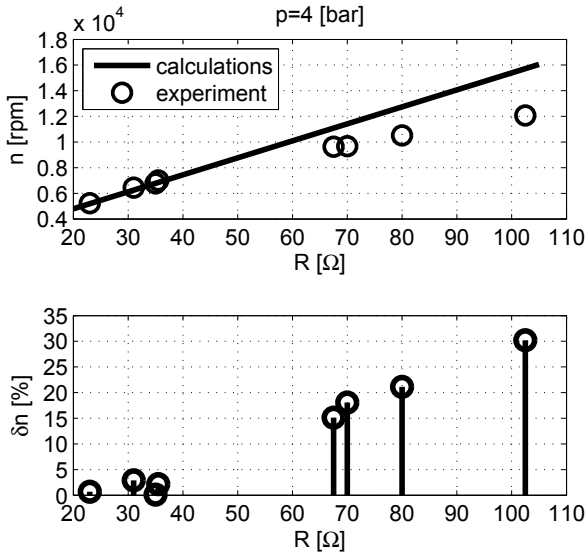

Figure 32: Rotational speed n of the microturbine set as a function of load resistance R, for constant pressure at turbine inlet p = 4 bar and relative error δn between experiment and calculations

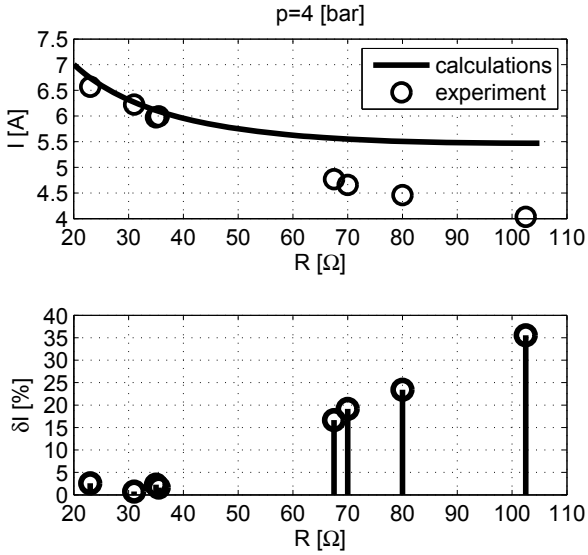

Figure 33: Electric current I of the microturbine set as a function of load resistance R, for constant pressure at turbine inlet p = 4 bar and relative error δI between experiment and calculations

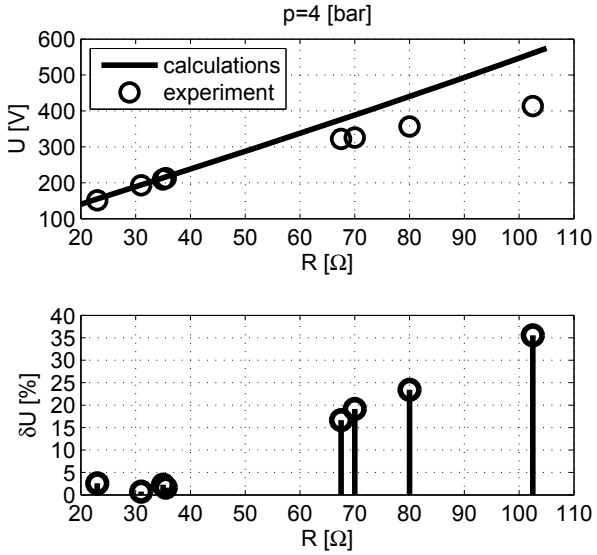

Figure 34: Electric voltage U of the microturbine set as a function of load resistance R, for constant pressure at turbine inlet p = 4 bar and relative error δU between experiment and calculations

with power 2800 W. The area of reliable operation of the microturbine set model is shown in the Figure 35.

6. Conclusions

The paper presents the mathematical model of a set consisting of microturbine, electric current generator with permanent magnets and rectifying unit. Model parameter values were determined based on experimental data. Series of calculations were performed to simulate the performance of the examined set in dynamically changing operating conditions, similar to those expected to take place in real operation (rapid load change, change of working medium pressure at turbine inlet). The obtained simulation data were compared with the results of experimental examination of the microturbine set. The calculated set responses to changes of input signals were identical in nature to those recorded in the experiment.

Within a large range of inlet pressure cases, the results of simulation calculations were close to the experimental data. The maximal relative differences between the experiment and the model did not exceed a few percent. An acceptable level of accuracy was obtained in a small range of load resis-

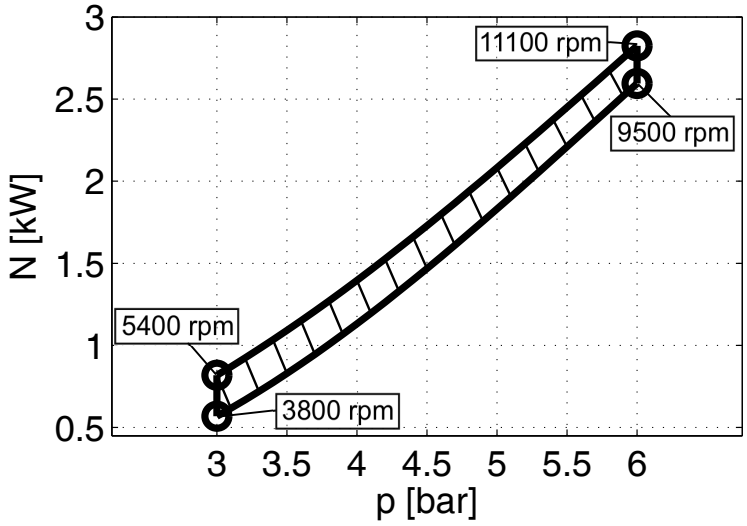

Figure 35: The area of reliable operation of the microturbine set model

tance. The presented results show that the use of the proposed model of microturbine set can ensure the accuracy of results which is sufficient for typical engineering calculations, for microturbine sets designed for operation with relatively small changes in electric load. This simplified model can be a useful tool for studying the various operational aspects of microturbine sets or for some engineering applications.

The considered microturbine system has not used any regulation method (for example voltage or rotational speed control). Control system have to be considered for completing energy generation using microturbine sets. The developed model can be also useful at the design stage of the control system.

The research based on the steam type microturbine set. However, the reported tests were performed using compressed nitrogen as the working medium. The conclusions formulated based on the obtained results can be extended to microturbine sets with turbines designed for supply with other working media.

Acknowledgements

This research did not receive any specific grant from funding agencies in the public, commercial, or not-for-profit sectors.

References

[1] Domachowski Z. Specificity of automatic control of microturbines (steam or gas -driven and expanders) in dispersed generation system of heat and electric power. Polish Maritime Research. 2009;Special issue S1:9-13.

[2] Amirante R, Tamburrano P. Novel, cost-effective configurations of combined power plants for small-scale cogeneration from biomass: Feasibility study and performance optimization. Energy Conversion and Management 2015;97:111-20.

[3] Dutra J C, Gonzalez-Carmona M A, Lazaro-Alvarado A F, Coronas A. Modeling of a Cogeneration System with a Micro Gas Turbine Operating at Partial Load Conditions. Journal of Sustainable Development of Energy, Water and Environment Systems 2017;5:139-50.

[4] Massardo A F, McDonald C F, Korakianitis T. Micro-turbine/Fuel-Cell Coupling for High-Efficiency Electrical-Power Generation. Transactions of the ASME, Journal of Engineering for Gas Turbines and Power 2002;124:110-16.

[5] Kosowski K. Steam and gas turbines. Principles of operation and design. France, Swiss, Great Britain, Poland: ALSTOM; 2007.

[6] Kosowski K. Steam and gas turbines. Power plants. France, Swiss, Great Britain, Poland: ALSTOM; 2007.

[7] Campanari S, Boncompagni L, Macchi E. Microturbines and Trigeneration: Optimization Strategies and Multiple Engine Configuration Effects. Journal of Engineering for Gas Turbines and Power 2004;126:92-101.

[8] Campanari S, Macchi E. Technical and Tariff Scenarios Effect on Microturbine Trigenerative Applications. Journal of Engineering for Gas Turbines and Power. 2004;126:581-89.

[9] Colombo L P M, Armanasco F, Perego O. Experimentation on a Cogenerative System Based on a Microturbine. Applied Thermal Engineering. 2007;27:705-11.

[10] Ho J C, Chua K J, Chou S K. Performance study of a microturbine system for cogeneration application. Renewable Energy 2004;29:1121-33.

[11] Logan Earl, Jr. Roy R. Handbook of Turbomachinery. Second Edition. New York: Arizona State University, Marcel Dekker Inc.; 2003.

[12] Stepniak D, Piwowarski M. Analysing selection of low-temperature medium for cogeneration micro power plant. Polish Journal of Environmental Studies 2014;23:1417-21.

[13] Saeid Mohammadzadeh Bina, Saeid Jalilinasrabady, Hikari Fujii. Energy, economic and environmental (3E) aspects of internal heat exchanger for ORC geothermal power plants. Energy 2017;140:1096-1106.

[14] Piwowarski M. Design analysis of ORC micro-turbines making use of thermal energy of oceans. Polish Maritime Research 2013;20:48-60.

[15] Mills D. Advances in solar thermal electricity technology. Solar Energy 2004;76:19-31.

[16] Dumont O, Dickes R, De Rosa M, et al. Technical and economic optimization of subcritical, wet expansion and transcritical Organic Rankine Cycle (ORC) systems coupled with a biogas power plant. Energy Conversion and Management 2018;157:294-306.

[17] Mikielewicz D, Wajs J, Ziolkowski P, Mikielewicz J. Utilisation of waste heat from the power plant by use of the ORC aided with bleed steam and extra source of heat. Energy 2016;97:11-19.

[18] Qiu G, Shao Y, Li J, Liu H, Riffat S. Experimental investigation of a biomass-fired ORC-based micro-CHP for domestic applications. Fuel 2012;96:374-82.

[19] Wajs J, Mikielewicz D. Cooperation of ORC installation with a gas boiler as a perspective co-generation system for households. Acta Energetica 2017;3:216-21.

[20] Liu X, Xu X, Liu C, et al. Heat transfer deterioration in helically coiled heat exchangers in trans-critical CO2 Rankine cycles. Energy 2018;147:1-14.

[21] Wajs J, Mikielewicz D. Effect of surface roughness on thermal-hydraulic characteristics of plate heat exchanger. Key Engineering Materials 2014;597:63-74.

[22] Wajs J, Mikielewicz D, Fornalik-Wajs E, Bajor M. Recuperator with microjet technology as a proposal for heat recovery from low-temperature sources. Archives of Thermodynamics 2015;36:48-63.

[23] Mikielewicz D, Mikielewicz J, Wajs J. Experiences from operation of different expansion devices for application in domestic micro CHP. Archives of Thermodynamics 2010;31:3-13.

[24] Xia G-D, Zhang Y-Q, Wu Y-T, et al. Experimental study on the performance of single-screw expander with different inlet vapor dryness. Applied Thermal Engineering 2015;87:34-40.

[25] Yun E, Kim HD, Yoon SY, Kim AC. Development and characterization of small-scale ORC system using scroll expander. Applied Mechanics and Materials 2013;291-294:1627-30.

[26] Lampart P, Kosowski K, Piwowarski M, Jedrzejewski L. Design analysis of Tesla micro-turbine operating on a low-boiling medium. Polish Maritime Research 2009;Special issue S1:28-33.

[27] Mikielewicz J, Piwowarski M, Kosowski K. Design analysis of turbines for co-generating micro-power plant working in accordance with organic Rankine's cycle. Polish Maritime Research 2009;Special issue S1:34-8.

[28] Piwowarski M, Kosowski K. Design analysis of combined gas-vapour micro power plant with 30 kW air turbine. Polish Journal of Environmental Studies 2014;23:1397-1401.

[29] Landelle A, Tauveron N, Haberschill P, et al. Organic Rankine cycle design and performance comparison based on experimental database. Applied Energy 2017;204:1172-87.

[30] Andrea Cavarzerea, Mirko Morini, Michele Pinelli, Pier Ruggero Spina, Anna Vaccari, Mauro Venturini. Experimental Analysis of a Micro Gas Turbine Fuelled with Vegetable Oils from Energy Crops. 68th Conference of the Italian Thermal Machines Engineering Association ATI2013.

[31] Macedo W, Monteiro L, et al. Biomass based microturbine system for electricity generation for isolated communities in amazon region, Renewable Energy 2016;91:323-33.

[32] Saiai P, Chaitep S, Bundhurat D, Watanawanyoo P. An Experimental Investigation of Vapor Generator Characteristics in a Low-pressure Turbine Engine. Indian Journal of Science and Technology 2014;7:1130-36.

[33] Wajs J, Mikielewicz D, Bajor M, Kneba Z. Experimental investigation of domestic micro-CHP based on the gas boiler fitted with ORC module. Archives of thermodynamics 2016;37:79-93.

[34] Kicinski J. Cogeneration in Small Scale – High Speed Microturbines Dynamic Analysis. Archives of Acoustics 2010;35;175-82.

[35] Kicinski J, Zywica G. Steam Microturbines in Distributed Cogeneration. Switzerland: Springer International Publishing Springer International Publishing; 2014.

[36] Lei Fu, Zhenping Feng, Guojun Li, Experimental investigation on overall performance of a millimeterscale radial turbine for micro gas turbine. Energy 2017;134:1-9.

[37] Zywica G, Drewczynski M, Kicinski J, Rzadkowski R. Computational Modal and Strength Analysis of the Steam Microturbine with Fluid-Film Bearings Journal of Vibration Engineering and Technologies 2014;2:543-49.

[38] Kosowski K, Wlodarski W, Piwowarski M, Stepien R. Performance Characteristics of a Micro-Turbine. Journal of Vibration Engineering and Technologies 2014;2:341-50.

[39] Ward De Paepe, Marina Montero Carreroa, Svend Bram, Alessandro Parente, Francesco Continoa. Experimental Characterization of a T100 micro Gas Turbine converted to Full Humid Air Operation. The 6th International Conference on Applied Energy 2014.

[40] Wlodarski W. Badania eksperymentalne mikroturbozespolow. Gdansk: Fundacja Promocji POiGM; 2016. [in Polish]

[41] Fethi O, Dessaint Louis-A, Kamal Al-Haddad. Modeling and simulation of the electric part of a grid connected microturbine. IEEE Xplore Conference: Power Engineering Society General Meeting 2004.

[42] Gaonkar D N, Patel R N. Modeling and simulation of microturbine based distributed generation system. Power India Conference IEEE 2006.

[43] Nayak S, Gaonkar D. Modeling and Performance Analysis of Microturbine Generation System in Grid Connected/Islanding Operation. International Journal of Renewable Energy Research 2012;2:750-57.

[44] Noroozian R, Abedi M, Gharehpetian G, Hosseini S. Modelling and Simulation of Microturbine Generation System for on-grid and off-grid Operation Modes. International Conference on Renewable Energies and Power Quality Valencia 2009.

[45] Torres E, Larragueta J, Eguia P, Mazon J, San Martin J, Zamora I. Dynamic Performance of a Microturbine Connected to a Low Voltage Network. Renewable Energy & Power Quality Journal 2008;1:468:73.

[46] Ali Chaibakhsh, Ali Ghaffari. Steam turbine model. Simulation Modelling Practice and Theory. 2008;16:1145-62.

[47] Ghazal Ghayem, Hamid Khaloozadeh. Modelling and Control of a Single Shaft Heavy Duty Industrial Gas Turbine Based on Operational Data. International Journal on Control Systems and Applications 2014;1:10.

[48] IEEE Committee Report. Dynamic Models for Steam and Hydro Turbines in Power System Studies. IEEE Transactions on Power Apparatus and Systems 1973;PAS-92:1904-15.

[49] Rowen W I. Simplified Mathematical Representations of Heavy-Duty Gas Turbines. Journal of Engineering for Power 1983;105:865-69.

[50] Ahn J B, Jeong Y H, Park D H. Development of High Speed PMSM for Distributed Generation Using Microturbine. The 30th Annual Conference of the IEEE Industrial Electronics Society Busan, Korea 2004.

[51] Belloni F, Chiumeo R, Gandolfi C, Villa A. Simulation model of a Permanent Magnet Synchronous Generator for grid studies. International Conference on Renewable Energies and Power Quality Cordoba 2014.

[52] Dehkordi A B, Gole A M, Maguire T L. Permanent Magnet Synchronous Machine Model for Real- Time Simulation. International Conference on Power Systems Transients Montreal 2005.

[53] Jari-Pascal Curty, Norbert Joehl, Francois Krummenacher, Catherine Dehollain, Michel J. Declercq. A Model for μ-Power Rectifier Analysis and Design. IEEE Transactions on Circuits and Systems. 2005;52:2771-79.

[54] Sergio Herraiz, Luis Sainz, Felipe Corcoles, Joaquin Pedra. A unified and simple model for uncontrolled rectifiers. Electric Power Systems Research 2005;74:331-40.

[55] Z. Xu, K. You, C. Zhang. Analytical Models of Power Losses of a Three phase AC-DC Rectifier for Hybrid Electric Vehicles. Energy Procedia 2016;88:978-84.

[56] Mohsen Rahimi. Modeling, control and stability analysis of grid connected PMSG based wind turbine assisted with diode rectifier and boost converter. Electrical Power and Energy Systems 2017;93:84-96.

[57] Pyrhonen J, Jokinen T, Hrabovcova V. Design of rotating electrical machines. John Wiley; 2008.

[58] Jones V H, Bonwick W J. Three-phase bridge rectifiers with complex source impedance. Proceedings of the Institution of Electrical Engineers 1975;122:630-36.

[59] Badami M, Ferrero M G, Portoraro A. Dynamic parsimonious model and experimental validation of a gas microturbine at part-load conditions. Applied Thermal Engineering 2015;75:14-23.

[60] Eguia P, Zamora I, Torres E, SanMartin J I, Moya M, Bruno J C, Coronas A. Modelling and Simulation of a Microturbine during Transient Events. Renewable Energy and Power Quality Journal 2010;1:354-59.